Electronic charge distribution in crystalline silicon

Moshe Deutsch
Department of Physics, Bar-Ilan University, Ramat-Gan 52100, Israel
(Received 20 March 1991)

Using the multipole-expansion formalism and recently published millielectron volt-level-accuracy x-ray structure factors, a detailed description of the crystal-bound silicon atom is derived. A 0.5% expansion of the L shell is detected, in addition to the known $\sim 6\%$ expansion of the M shell. A nonrigid thermal motion of the atom is also found, with the valence charge vibrating with a much reduced amplitude. Strong evidence is also found for a twofold reduction over the theoretical prediction for the magnitude of the anharmonic force constant in the effective one-atom potential. The R factor of our improved model is only 50% that of the best previously published one, and the goodness of fit is close to unity, indicating that the model exhausts the accuracy of the measured data. Deformation and valence-charge-density maps are presented and found to be in good agreement with previous results. Wave-function- and model-specific influences such as wave-function quality and relativistic and exchange-potential effects are also discussed. It is concluded that their influence on the conclusions of the present study is marginal.

I. INTRODUCTION

The electronic structure of crystalline silicon has received extensive experimental and theoretical attention over the past two decades. The availability of large, perfect silicon crystals allowed for the development and application of sophisticated dynamical techniques for measuring the structure factors of silicon to millielectron volt-level accuracies[1-5] better by 1 order of magnitude or more than any other crystal. Furthermore, accurate measurements of the important "forbidden" structure factors, which provide direct information on deformation electron densities, could be done.[6-8] These measurements allowed for very detailed crystal-structure determinations[9-14] and provided a highly accurate yardstick against which *ab initio* theoretical crystal-binding calculations[15-20] could be tested. The theoretical activity was further spurred by renewed interest in band-structure calculations,[15-18] linear combination of atomic orbitals (LCAO),[17(b)] and linear muffin-tin orbital[20] (LMTO) methods. From these studies emerged an unprecedentally detailed qualitative and quantitative description of the crystal-bound silicon atom. Some of its noteworthy features are a $\sim 6\%$ expansion of the valence M shell,[1,11,12,14] nonspherical charge distortions of octopolar and hexadecapolar symmetries,[1,11-14] and a double-peaked valence charge density along the covalent silicon-silicon bond.[12,16] On the theoretical side, the Kohn-Sham local-density-functional approach[21] proved to be very successful in predicting details of the crystalline structure at the atomic level, as well as macroscopic static (bulk modulus and elastic constants[16,19]) and dynamic (phonon frequencies[20(a),(c)]) properties. The hard-core pseudopotential was shown to yield better valence charge densities than those of the traditional soft-core one.[15]

Several important issues, however, still remain outstanding. The Debye parameter B derived from high-order ($1<\sin\theta/\lambda<1.6$ Å^{-1}) x-ray structure factors[5,22] was found to be significantly lower than that of low-order reflections, a result also supported by electron channeling measurements.[23] These results cast doubt[22] on the validity of the rigid-atom approximation, hitherto employed in all structure determinations, in accounting for the thermal motion of the atoms at millielectron volt-level accuracies. Further, Spackman,[12] in his recent detailed charge-density analysis, detected a consistent trend in the fit residuals, which he ascribed to a deformation of the core L shell. The accuracy of the data available to him was, however, insufficient to allow for a determination of the nature and magnitude of the deformation. Another controversial issue is the existence and magnitude of an anharmonic term in the effective one-atom potential. To the lowest anharmonic term, the effective potential is given by[9]

$$V(\mathbf{r})=V_0(\mathbf{r})+\gamma(x^2+y^2+z^2)/2+\beta xyz\ , \tag{1}$$

where γ and β are the harmonic and anharmonic force constants, respectively. While γ is related to B and can be, therefore, determined accurately, the smaller β is much more difficult to determine and estimates vary by more than a factor of 4.[12,5] Several "forbidden" reflection neutron and x-ray measurements of Batterman and co-workers[7,8] yield values ranging from 1.38 to 3.38 eV/Å^3, while x-ray measurements[1,5,22] indicate an upper limit of ~ 0.8 eV/Å^3. The ambiguity in the neutron results parallels that of the separation of the various contributions to the "forbidden" 442 and 622 structure factors.[8,12]

Recently, a consolidated set of structure factors was published, and its accuracy carefully assessed.[2] The accuracy of this set, at least twice that of previous data,[9] allowed us to address the issues above within the framework of the Dawson-Stewart-Coppens[9,24-27] multipole expansion formalism and obtain definite rulings on some of them. Our results, presented in the following, reveal

an expansion of ~0.5% of the core L shell of the atom in addition to the above-mentioned ~6% expansion of the valence M shell. A much smaller B value is found for the valence shell as compared to that of the core, indicating a reduced thermal motion. The x-ray derived upper limit on β is strongly supported by our results.

The data set, the models employed in the analysis, and the results obtained are described in Secs. II–IV. A comparison of the values derived from our results for the 442 and 622 "forbidden" structure factors and the measured values is also presented. Our conclusions are given in Sec. V.

II. MEASURED DATA

Five high-precision sets of structure factors, $f_m(hkl)$, measured in three independent experiments are available at present. We use only those reflections which have been measured at least twice. The two sets of Aldred and Hart,[1] measured with Mo $K\alpha$ and Ag $K\alpha$ radiations using a wedge-Pendelösung method with film detection, include 15 such reflections. These sets, which were for many years the "standard of the trade" and employed repeatedly in numerous studies,[11–14,16,19,22,26] were recently[2] corrected for the (minute) effects of strain gradients and adjusted to 20°C. The two sets of Teworte and Bonse,[3] measured with the same radiations and employing thin-crystal Laue-case rocking curves, include 16 reflections. The last set, that of Saka and Kato,[4] measured using the rotating-plate thickness-Pendelösung technique at a wavelength of 0.4 Å, includes 17 reflections. A careful analysis[2] indicates that all five sets have similar average accuracies of 3–5 millielectrons, as claimed by all but Saka and Kato.[4] Their estimate of a tenfold higher accuracy seems to be overoptimistic. All sets were corrected for nuclear scattering using $f_N = 0.0038e$ and for anomalous dispersion using experimentally derived f' values[28] of accuracy commensurate with that of the f_m data. The important "forbidden" $f_m(222)$, measured by Alkire, Yelon, and Schneider[6] to ± 1 me, was also included in our data set. The anharmonic contribution to $f_m(222)$ is negligible even for the largest value of β given above. For 442 and 622, however, this is a major contribution. In view of the ambiguity in the value of β discussed above, the measured[7,8] $f_m(442)$ and $f_m(622)$ were not included in our data set, but used as control values as discussed in Sec. IV D. The f_m set of Hattori *et al.*[30] was also excluded due to insufficient accuracy.[12,13] The only available set of high-accuracy, high-order f_m values, measured by Deutsch and Hart,[5] was excluded as well, since high-order reflections are not influenced by bonding effects which are the subject of the present study. Furthermore, we wanted to confirm the nonrigid thermal motion of the silicon atom, detected in that study as discussed above, from independently measured structure factors. A preliminary fit, in which the high-order structure factors were included along with the low-order ones, indicated that they strongly bias the fit in that respect.

Thus, the consolidated f_m set used in the present study was generated from an average of the five f'- and $-f_N$-corrected sets discussed above, and $f_m(222)$ of Alkire *et al.*[6] The estimated standard errors (ESD's) were calculated, using standard methods,[29] from those of the individual sets, excluding the estimated errors of Saka and Kato[4] for reasons mentioned above. A comparison of the resultant ESD's to those of the original sets shows an average twofold increase in accuracy. The f_m set is listed in Table I along with its ESD's and other relevant data. It includes 18 values in the range $0 < \sin\theta/\lambda < 1.04$ Å^{-1}, out of the 51 possible reflections in this range.

TABLE I. Measured structure factors f_m, their estimated standard deviations σ_m, and phase factors for hkl reflections employed in this study.

hkl	$\sin\theta/\lambda$ (Å^{-1})	a	b	c	d	f_m (e/atom)	σ_m (e/atom)
111	0.159 48	1	−1	−1	−1	10.602 5	0.002 9
220	0.260 42	1	0	0	−1	8.388 1	0.002 2
311	0.305 37	1	1	1	−1	7.681 4	0.001 9
222	0.318 95	0	−1	−1	0	0.182 0	0.001 0
400	0.368 29	1	0	0	−1	6.995 8	0.001 2
331	0.401 34	1	−1	−1	−1	6.726 4	0.002 0
422	0.451 07	1	0	0	−1	6.112 3	0.002 2
333	0.478 43	1	1	1	−1	5.780 6	0.002 1
511	0.478 43	1	−1	−1	−1	5.790 6	0.002 7
440	0.520 85	1	0	0	−1	5.332 4	0.002 0
444	0.637 90	1	0	0	−1	4.123 9	0.001 8
551	0.657 54	1	−1	−1	−1	3.934 9	0.003 4
642	0.689 02	1	0	0	−1	3.655 8	0.005 4
800	0.736 59	1	0	0	−1	3.248 5	0.003 4
660	0.781 27	1	0	0	−1	2.914 3	0.001 6
555	0.797 38	1	−1	−1	−1	2.800 9	0.002 1
844	0.902 13	1	0	0	−1	2.150 6	0.002 4
880	1.041 70	1	0	0	−1	1.532 5	0.002 6

III. THE MODEL

The at-rest spherical free-atom charge density ρ_c deforms to follow site symmetry as the silicon atom becomes crystal bound. According to the Dawson-Stewart-Coppens formalism,[9,24-27] these deformations are expanded in real spherical harmonics. Since the deformations are small, only terms up to the hexadecapole need be retained. For silicon, having a diamond structure, the only nonvanishing terms are[9] the octopole, ρ_3, the hexadecapole, ρ_4, and the monopole. The last of these represents a radial expansion or contraction of the shell and is accounted for[26] by scaling the position vector $\mathbf{r}$ of the relevant shell by some value κ. The model charge density is thus given by

$$\rho_c(\mathbf{r})=\sum_{nl}\kappa_{nl}^3\rho_{nl}(\kappa_{nl}\mathbf{r})+O\rho_3(\mathbf{r})+H\rho_4(\mathbf{r}) , \tag{2}$$

where O and H are the respective populations and nl designates the shell. The Slater-type orbitals of Clementi,[31] extensively used in previous studies, were employed to represent $\rho_{nl}(r)$:

$$\rho_{nl}(r)=(4\pi)^{-1}P_{nl}\left[\sum_i N_i C_i r^{n_i-1}\exp(-\xi_i r)\right]^2 , \tag{3}$$

where P_{nl} is the shell population,

$$N_i=(2\xi_i)^{n_i+1/2}/[(2n_i)!]^{1/2}$$

and the constants n_i, ξ_i, and C_i are given in Ref. 31 for each shell. Following Price *et al.*[11] (PMM), Spackman,[12] Hansen and Coppens[26] (HC), and others, the radial functions of both higher multipoles were taken as single $r^n\exp(-\alpha r)$ functions, yielding[11,26]

$$\rho_3(\mathbf{r})=ON_o r^{n_o}\exp(-\alpha_o r)(2xyz/r^3) \tag{4a}$$

and

$$\rho_4(\mathbf{r})=HN_h r^{n_h}\exp(-\alpha_h r)[160/(27\sqrt{3}\pi)]\times[(x^4+y^4+z^4)/r^4-\tfrac{3}{5}] . \tag{4b}$$

Complying with common practice,[11,12] based on comparative studies by PMM and Spackman, we set $n_o=n_h=n=4$ and $\alpha_o=\alpha_h=\alpha$. The normalization factors are $N_o=N_h=\alpha^{n+3}/(n+2)!$. The exponential model given by Eqs. (1)–(4) is denoted by EX in the following.

The corresponding stationary scattering amplitudes $f_c(\mathbf{k})$ are obtained by Fourier transforming ρ_c, yielding[26]

$$f_c(\mathbf{k})=\sum_{nl} f_{nl}(\mathbf{k}/\kappa_{nl})+Of_3(\mathbf{k})+Hf_4(\mathbf{k}) , \tag{5}$$

where $|\mathbf{k}|=k=(2\pi/a_0)(h^2+k^2+l^2)^{1/2}$ and a_0 is the lattice constant. The terms in Eq. (5) are

$$f_{nl}(k)=\sum_{i,j} P_{nl}C_iC_jN_iN_j\mathcal{J}_{n_i+n_j,0}(k,\xi_i+\xi_j) , \tag{6a}$$

$$f_3(\mathbf{k})=-OA_3(8\pi)N_o\mathcal{J}_{n_o+2,3}(k,\alpha_o) , \tag{6b}$$

and

$$f_4(k)=HA_4[640/(27\sqrt{3})]N_h\mathcal{J}_{n_h+2,4}(k,\alpha_h) . \tag{6c}$$

For a given hkl reflection,[9]

$$A_3=hkl/(h^2+k^2+l^2)^{3/2}$$

and

$$A_4=[(h^4+k^4+l^4)/(h^2+k^2+l^2)^2-\tfrac{3}{5}]$$

and $\mathcal{J}_{m,n}(s,z)$ is given by

$$\mathcal{J}_{m,n}(s,z)=\int_0^\infty r^m j_n(sr)\exp(-zr)dr \tag{7a}$$

$$=K\,{}_2F_1((n-m+1)/2,(n-m+2)/2;(2n+3)/2;-(s/z)^2) , \tag{7b}$$

where $j_n(x)$ are the spherical Bessel functions of the first kind, ${}_2F_1(a,b;c,x)$ is the Gauss hypergeometric series, and

$$K=(s/z)^n[(n+m)!/(2n+1)!!]z^{-(n+1)}\times[1+(s/z)^2]^{-1} .$$

Closed-form expressions for $\mathcal{J}_{m,n}(s,z)$ were recently published by Su and Coppens[32] for $m\le 8$ and $n\le m-1$.

We now include the effect of thermal motion on the charge distribution by invoking the convolution approximation.[9] The at-rest distribution is convoluted with an atomic smearing function, the form of which depends on the effective potential seen by the vibrating atom. Fourier transforming the temperature modified density to obtain f yields temperature factors multiplying $f_c(hkl)$ of Eq. (5). For the potential of Eq. (1), Dawson[9] has shown that two temperature factors are obtained:

$$T_h(k,B)=\exp[-k^2k_BT/(2\gamma)]=\exp[-Bk^2/(4\pi)^2] , \tag{8a}$$

which is the well-known harmonic Debye-Waller factor, and

$$T_a(k,\beta,B)=T_h(k,B)[2\pi/(\gamma a_0)]^3(k_BT)^2\beta hkl , \tag{8b}$$

which is the anharmonic temperature factor. Note that the last is much smaller than the first. Even for the largest estimate of β given above, $T_a/T_h\approx 2.7\times10^{-5}hkl$ at room temperature. Hence, the difficulty in detecting its contribution even in the most accurate low-order f_m data.

Taking the phase factors a, b, c, and d, calculated by Dawson[9] and listed in Table I, into account, and allowing for a different Debye-Waller parameter for each shell,[22] the temperature-modified model $f_c(k)$ becomes

$$f_c(k)=\sum_{nl} f_{nl}(k/\kappa_{nl})[aT_h(k,B_{nl})+cT_a(k,\beta,B_{nl})]$$
$$+Of_3(k)[bT_h(k,B_o)+dT_a(k,\beta,B_o)]$$
$$+Hf_4(k)[aT_h(k,B_h)+cT_a(k,\beta,B_h)]\ . \quad (8c)$$

This is the general expression for the models used in the present study.

The temperature-modified $f_c(hkl)$ of Eq. (8) is now least-squares fitted to the measured $f_m(hkl)$ values. The refined fit parameters are then inserted into $\rho_c(\mathbf{r})$ to determine the charge distribution. In principle, a different B_{nl} and κ_{nl} can be assigned to each shell.[22] However, to keep the number of fit variables manageable and to comply with more conservative practices,[5,11] only two of each were allowed; B_1 ($n=1,2$ shells), B_2 ($n=3$), κ_1 ($n=2$), and κ_2 ($n=3$) with $B_o=B_h=B_2$. This allows for a different thermal motion for the core and valence shells, and a radial expansion of both the L and M shells. Thus, the maximal number m of fit parameters in the present model is 8: O, H, α, B_1, B_2, κ_1, κ_2, and β. However, subsets of different size and choice ($4\leq m\leq 8$) were tested systematically to determine the relative importance and manner of influence of the various parameters. The best model, discussed below, was obtained using seven parameters.

IV. RESULTS AND DISCUSSION

A. Fit results

Details of the various fits along with their goodness-of-fit (GOF) and R factors are given in Table II. Note first that a model neglecting the M-shell expansion (a), detected in earlier studies, results in an unacceptably high GOF, which is reduced by a factor of 2 upon the inclusion of the expansion (b). Thus, the ~6% expansion of the M shell is reconfirmed. The model employed in $b-d$, which imposes the rigid-atom approximation[9] (i.e., a single B) and allows for an expansion of the M shell in addition to the higher multipolar deformations, is essentially the same as the most detailed models of previous studies, notably, those of Spackman, PMM, and HC. In an effort to resolve the ambiguity discussed above in the value of β, the fits of each model were repeated for $\beta=0$, 1.67, 3.38 eV/Å^3, the x-ray prediction, and two of the neutron values, respectively. The parameter values obtained, listed in Table III, are all in good agreement with those of Spackman and PMM. The GOF~5, however, clearly shows scope for improvement. Note that the R and GOF factors for the three values of β are roughly equal and show no preference for any of the values. If variation of β is allowed in the fit, convergence deteriorates, the final $\beta\approx 0$ obtained has a rather large ESD, and, more significantly, no reduction in R or GOF results. The model of $b-d$ is therefore insensitive to the value of β, a conclusion also reached by Spackman (see his *note added in proof*).

Relaxing now the rigid-atom requirement by taking either $B_1\neq B_2$ (fits $e-g$) or keeping it but allowing an L-shell expansion through $\kappa_1\neq 1$ (fits h-j), a reduction of

TABLE II. The parameters varied and their number m, the anharmonic force constant β used, and the R and goodness-of-fit (GOF) factors obtained in the various model fits. Note the dramatic reduction in R and GOF in models $p-r$ which allow for nonrigid atomic thermal motion and the expansion of the L shell.

	a	b	c	d	e	f	g	h	i	j	p	q	r
Var:	$B_1=B_2$	$B_1=B_2$	$B_1=B_2$	$B_1=B_2$	B_1,B_2	B_1,B_2	B_1,B_2	$B_1=B_2$	$B_1=B_2$	$B_1=B_2$	B_1,B_2	B_1,B_2	B_1,B_2
	α,H,O	α,H,O	α,H,O	α,H,O	α,H,O	α,H,O	α,H,O	α,H,O	α,H,O	α,H,O	α,H,O	α,H,O	α,H,O
		κ_2	κ_2	κ_2	κ_2	κ_2	κ_2	κ_1,κ_2	κ_1,κ_2	κ_1,κ_2	κ_1,κ_2	κ_1,κ_2	κ_1,κ_2
m	4	5	5	5	6	6	6	6	6	6	7	7	7
β (eV/Å^3)	0	0	1.67	3.38	0	1.67	3.38	0	1.67	3.38	0	1.67	3.38
R (%)	0.226	0.166	0.159	0.162	0.087	0.093	0.111	0.090	0.089	0.098	0.036	0.045	0.062
GOF	10.5	5.75	5.57	5.57	3.250	3.23	3.59	2.82	2.83	3.13	1.20	1.57	2.35

TABLE III. Parameter values refined for the "standard" model $b-d$ and the improved one $p-r$. The second line of each entry lists the standard deviation in the last digits of the value given above it. Note the reduction in the standard deviation of all parameters in $p-q$ as compared to $b-d$.

	b	c	d	p	q	r
β (eV/Å^3)	0	1.67	3.38	0	1.67	3.38
B_1 (Å^2)	0.4658	0.4663	0.4667	0.4585	0.4593	0.4599
	19	10	19	15	10	24
B_2 (Å^2)				0	0	0
				0.11	0.11	0.14
α (a.u.$^{-1}$)	2.502	2.487	2.472	2.435	2.425	2.413
	79	53	56	10	5	14
κ_1				0.9949	0.9951	0.9951
				6	2	10
κ_2	0.9501	0.9481	0.9461	0.9382	0.9367	0.9350
	95	95	99	15	10	16
H (e)	−0.1320	−0.1361	−0.1410	−0.1270	−0.1307	−0.1349
	200	240	300	57	14	77
O (e)	0.4310	0.4340	0.4370	0.4484	0.4499	0.4521
	330	300	310	62	36	70

$\sim 40\%$ in R and GOF is obtained. R indicates a much better fit for all β and a slight preference for low values of β is observed. The GOF≈ 3, however, indicates that the accuracy of the data is still not exhausted. We include, then, both effects and obtain the results shown under $p-r$. The drastic reduction in R shows that the data strongly supports the effects postulated. The refined parameter values are listed in Table III. Note that the ESD's obtained for the parameters are much smaller than those of $b-d$, lending further support for this model. Unlike the five-parameter models, $b-d$, a clear preference for $\beta \approx 0$ is seen, indicating a much reduced upper limit on anharmonic effects. The implications of this, and the magnitude of the limit, are discussed below.

The results listed in Table II indicate, then, that model p is the best model of this study. Its R factor is only $\sim 35\%$ and $\sim 50\%$ of those of Spackman and PMM, the best models published to date. The GOF is close to 1, indicating that the accuracy of the f_m data is practically exhausted, and the inclusion of additional effects through more fit parameters will probably result in an increase in R and GOF. The fit residuals, $f_m - f_c$, are all within the limits of $\pm 2\sigma_m$ of the data and are randomly distributed. No systematic trend like that observed by Spackman in his residuals can be detected. The 6.2% expansion of the valence shell agrees well with previous values ranging from[1] 6.8% to[26] 4.4%. The small 0.5% L-shell expansion is detected here for the first time, and is in concord with the L-shell deformation suggested by Spackman. α is close to 2.358 a.u.$^{-1}$ of Spackman and 2.2–2.7 a.u.$^{-1}$ of PMM. While B_1 is somewhat lower than 0.4676(14) Å^2 of PMM and 0.4632(11) Å^2 of Spackman, it agrees well with 0.461(3) Å^2 of Aldred and Hart[1] and is slightly larger than Fehlmann's[14] 0.4515(27) Å^2. We may therefore conclude that the general agreement with previous refinements is fairly good, bearing in mind that strict "within error" agreement cannot be expected due to the difference in the models.

A significant feature of our model is the allowance made for a possible deviation from the rigid-atom approximation. The fact that we obtain $B_2 \neq B_1$ clearly demonstrates that this approximation is no longer justified at millielectron volt-level accuracies. This supports earlier suggestions (see the Appendix in PMM), electron channeling,[15] and our high-order f_m x-ray[12,14] results. The value obtained, $B_2 = (0 \pm 0.11)$ Å^2, is considerably lower than the theoretically suggested[33] limit of $B_{\text{bond}} = 0.5 B_{\text{core}} \approx 0.23$ Å^2, which is based on the assumption of completely uncorrelated motion of nearest-neighbor atoms. Now, $B_2 = 0$ is in perfect agreement with the temperature dependence measured by Trucano and Batterman[8(c)] for the "forbidden" $f_m(422)$ which is dominated by the bonding charge ρ_3. The temperature dependence of the strongest "forbidden" reflection, 222, as measured by Batterman and co-workers[7,34] also indicates that $B_{\text{bond}} < B_{\text{core}}$ and is consistent with $B_{\text{bond}} \approx 0$, although a higher value is also possible.[7] Since a strict zero value is physically unrealistic, our result should be taken to indicate that $B_2 \leq 0.11$ Å^2, which amounts to a $\sim 30\%$ reduction in the thermal vibrational amplitude relative to the theoretical prediction. Allowing for more[22] than two independent B_{nl} could perhaps bring the various observations and predictions into better agreement when more accurate data becomes available.

Turning now to the question of the upper limit on β, we note that when β is also allowed to vary as a fit parameter in any of the $p-r$ fits, a final $\beta = (0 \pm 0.7)$ eV/Å^3 is obtained. As discussed above for B_2, this does not mean a strict $\beta = 0$, but rather that $\beta \leq 0.7$ eV/Å^3. This upper limit is in good agreement with the previous x-ray results[1,5,22] which yield $\beta \leq 0.8$ eV/Å^3. It is, however, considerably lower than the values derived from neutron, and combined x-ray-neutron, measurements of the temperature dependence of "forbidden" reflection intensities.[7,8,34] Nevertheless, our limit of $\beta \leq 0.7$ eV/Å^3 represents a confidence interval of one standard devia-

tion. Adopting a more conservative confidence interval of 2σ would put our result barely in agreement with the lowest "forbidden" reflection result, but not with the higher values. Since the forbidden reflections are very weak, their intensity determination requires correction for multiple reflection effects, often larger than the signal itself. Furthermore, the extraction of β from the temperature dependence of the intensities requires the assumption that the at-rest deformation density itself is temperature independent over a range of $\sim 1000\,^{\circ}\mathrm{C}$ and all temperature dependence is included in the temperature factors. Small deviations from the expected T^2 dependence detected, especially around room temperature,[7,8(a)] indicate that this may not be the case. Also, the neutrons probe the thermal motion of the nucleus while the x rays, that of the electrons. Thus, either a rigid-atom approximation or a division into core and bond charges, where the core moves rigidly with the nucleus, has to be invoked when determining the value of β from the combined measurements. Evidence that neither approximation may be valid at the millielectron accuracy level is discussed in Refs. 22 and 23. Furthermore, different measurements of the Batterman group yield different conclusions on this point. Consequent to these difficulties, even the very sophisticated and careful "forbidden" reflection measurements of Batterman and coworkers[7,8,34] yield values ranging from 1.38 to 3.38 eV/Å^3. The bond charge densities obtained for the higher-order "forbidden" 442 and 622 reflections by Spackman in his recent comprehensive refinement[12] strongly supports $\beta=3.38$ eV/Å^3. Clearly, further work is indicated to resolve the discrepancies among these values as well as our lower limit. It should, however, be noted that the conclusions concerning the L-shell expansion and the nonrigid thermal motion remain in effect even if the high value of β is adopted. This is clearly seen by intercomparing the results of the fits done for $\beta=3.38$ eV/Å^3, i.e., d, g, j, and r, and noting the drastic reduction in R and GOF achieved by including the above mentioned effects.

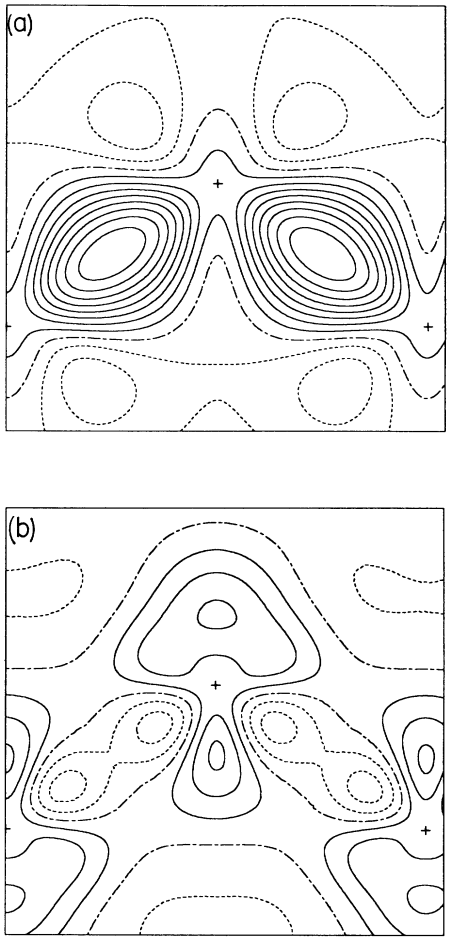

FIG. 1. At-rest charge density maps in the 110 plane of silicon. (a) Deformation density $\rho_{\mathrm{def}}=\rho_3+\rho_4$ for model p. Contour interval is 0.025 e/Å^3. (b) Difference in ρ_{def} between models p and b. Contour interval is 0.0025 e/Å^3. Map area is 4×4 Å^2 for both figures. The zero level is indicated by dash-dotted line and negative levels by dashed lines. The atoms are marked by +.

B. Deformation density

The at-rest charge deformation density $\rho_{\mathrm{def}}=\rho_3+\rho_4$ in the plane of bond, (110), obtained from fit p is given in Fig. 1(a). Its general shape is similar to those of PMM and Spackman; an elliptical peak elongated both in the bond direction and normal to it, and an almost circular dip behind the atoms. The main difference is that, in our model, the elongation is larger in the bond direction while, for Spackman and PMM, the elongation is larger in the normal direction. Our result demonstrates that a $\langle 111\rangle$-elongated bonding charge can be obtained even with a nonzero M-shell expansion, contrary to PMM's conclusion. We find a midbond peak of 0.221 e/Å^3 height and a $-0.068e$/Å^3 deep dip at $R=0.96$ Å behind the atoms. This is in perfect agreement with Scheringer's[13] 0.22 e/Å^3 and slightly higher than the corresponding 0.206 and -0.090 e/Å^3 of Spackman. Most of the difference results from our ~ 0.020 e/Å^3 larger ρ_4 contribution at the peak and dip regions, due to our larger H value, -0.1270 e, as compared to the average -0.102 e of Spackman. The lower peak height of 0.13 e/Å^3 obtained by PMM was shown[12,13] to result from the exclusion of the "forbidden" $f_m(222)$, whose contribution of ~ 0.07 e/Å^3 would bring the peak height to ~ 0.20 e/Å^3 in reasonable agreement with the values obtained by us and others.

The only theoretical *deformation* density map published to date (to the best of our knowledge), that of Wang and Klein,[19] shows an almost rectangular shape elongated in the direction normal to the bond. This shape is not supported by any of the experimental studies, including ours, although the elongation direction agrees with PMM and Spackman but not with our results. The peak value, ~ 0.16 e/Å^3, is too low but the -0.08 e/Å^3 dip behind the atom is in good agreement with our and Spackman's results. Inspection of the difference map given in Fig. 1(b) reveals that, on going

from the "standard" model b to our improved model p, some of the charge density is removed from the bond ends close to the atoms and is redistributed in the $\langle 001 \rangle$ direction both above and below the atom, leaving the peak and dip heights virtually unchanged. The changes are, however, small and involve ~ 8 me/Å^3 at most.

C. Valence density

The valence charge density in the (110) plane is shown in Fig. 2. The characteristic square shape with twin peaks along the bond is clearly seen. The valence charge density derived here is in excellent agreement with that of Spackman. The elliptic, single-peaked shape obtained using Fourier summation by Yang and Coppens[10] were shown by Spackman and Scheringer[13] to result from the inclusion of the less accurate structure factors of Hattori *et al.*[30] in his data set. Along the bond direction we obtain peak and saddle heights of 0.602 and 0.596 e/Å^3, respectively. This compares well with the corresponding average values of 0.597 and 0.576 e/Å^3 of Spackman. The different saddle heights result, again, from ρ_4. The crescent-shaped peaks behind the atoms are 0.341 e/Å^3 high, somewhat lower than the average 0.393 e/Å^3 of Spackman but in good agreement with some of the theoretical results.[15,19] Our peak-to-saddle height difference, 0.006 e/Å^3, is smaller by a factor of 2–3 than that of the standard model as given in fit b (0.012 e/Å^3) and by Spackman (0.020 e/Å^3). This considerably improves the agreement with the numerous theoretical results,[15–20] almost all of which predict a flat midbond charge density. In the few[16(c),19,20(b),20(c)] which exhibit a double-peaked shape, the saddle seems extremely shallow. Unfortunately, no numerical values are quoted by the authors. The difference map given in Fig. 2(b) indicates, again, that, on going from the standard model b to the improved one p, some of the charge is removed from the bond ends and redistributed closer to, and around, the atom. The maximal density changes are ~ 20 me/Å^3, about 2–3 times those found in the deformation density.

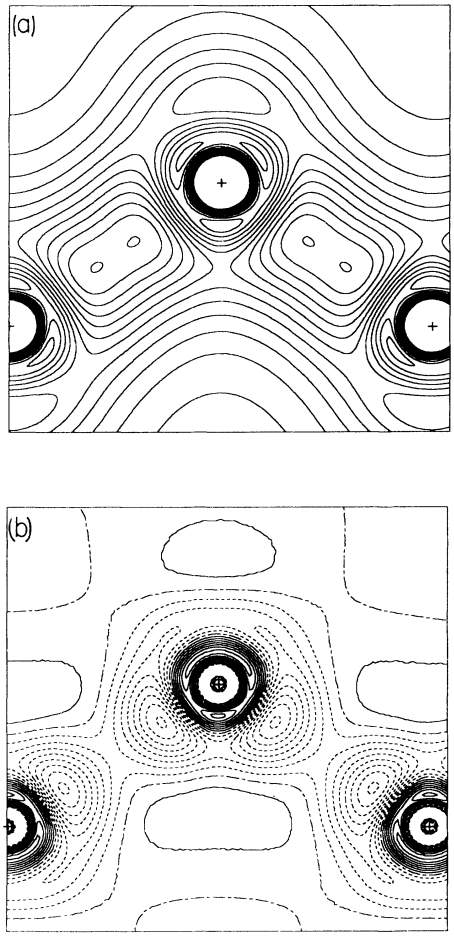

FIG. 2. Same as Fig. 1 but for the valence density. Contour interval for (a) is 0.05 e/Å^3.

The large number of theoretical valence density maps published for silicon makes a comprehensive comparison of our results with theory impractical. We will therefore restrict our comments mostly to a few of the more recent studies. The peak heights predicted range from[19] 0.535 to[17(a)] 0.65 e/Å^3, and generally agree with our result. The nonlocal pseudopotential calculations of Zunger and Cohen,[16(b)] 0.600 e/Å^3, yield the best agreement. The new LMTO (Ref. 20) and LCAO [Ref. 17(a)] methods tend to underestimate the bond peak height, and yield values of 0.55–0.56 e/Å^3. They are, however, rather successful in reproducing the general shape of the valence charge density. In particular, Weyrich[20(c)] and Methfessel *et al.*[20(a),(b)] reproduce well the double-peaked shape of the bond along the $\langle 111 \rangle$ direction, following the Hamann[15] demonstration that the single peaked charge density obtained in earlier calculations is an artifact due to the soft-core pseudopotential employed. Andersen *et al.*[20(d)] show that a similar effect, although of a smaller magnitude, results from adopting the pure-*lm* approximation for the tight-binding orbitals in the LMTO calculations. The full-potential results of Hamann[15] reproduce extremely well our charge density in the difficult regions close to the atom, where a slight decrease in density along the bond is seen accompanied by a small increase in density close to the atom in the $\langle 001 \rangle$ direction both below and above it. Finally, Yin and Cohen[16(b)] obtain a saddle-to-peak difference of 10 me/Å^3 in good agreement with our 6 me/Å^3, although their peak height of 0.575 e/Å^3 is somewhat lower than our 0.602 e/Å^3.

To conclude, the theoretical calculations best reproducing our results seem to be those of Zunger and Cohen[16(c)] and Yin and Cohen.[16(b)] The LMTO results of Weyrich[20(c)] and Methfessel *et al.*[20(a),(b)] while in excellent agreement as regards the shape of the charge density maps, need to be modified to yield better quantitative agreement in the bond regions.

D. The forbidden 442 and 622 reflections

Batterman and co-workers[7,8] measured, in a series of *tour de force* experiments, the structure factors of the three lowest-order basis-forbidden reflections (222, 442,

and 622) of silicon. Their integrated intensities are 3 (222) to 6 (442, 622) orders of magnitude smaller than low-order-allowed reflections, rendering their measurement an extremely demanding task. The finite scattering amplitudes f of these reflections are due to two effects. One is the antisymmetric bond charge deformation ρ_3, and the second is the anharmonic thermal motion of the centrosymmetric charge distribution $\sum_{nl}\rho_{nl}+\rho_4$. Free volume considerations,[8(d)] strongly supported by the experimental results,[8(a)-(d)] indicate that the two contributions have opposite signs. Taking into account the relevant temperature factors, the temperature-modified structure factors per atom for these reflections can be written as

$$F(hkl)=F_{\text{bond}}-F_{\text{anh}} \tag{9a}$$

$$=Of_3(hkl)T_h(hkl,B_o) - \left[\sum_{nl} f_{nl}(hkl)T_a(hkl,\beta,B_{nl}) + Hf_4(hkl)T_a(hkl,\beta,B_h)\right], \tag{9b}$$

where T_a and T_h are the anharmonic and harmonic temperature factors, respectively, of Eqs. (8a) and (8b). Thus, knowledge of β and the centrosymmetric structure amplitudes allows the separation of the measured structure factor F into the bond and anharmonic components of Eq. (9a). Equation (9b), on the other hand, can be used to synthesize the same quantities from fitted models. Note that the relative magnitude of the two components in Eq. (9) varies strongly with hkl. 222 is dominated by F_{bond} and F_{anh} is negligible.[7] By contrast, Batterman and coworkers[8] found that, at room temperature, $F_{\text{bond}}(442)$ dominates over $F_{\text{anh}}(442)$ by a factor of 2 only, while $F_{\text{bond}}(622)$ and $F_{\text{anh}}(622)$ have roughly the same magnitude and almost cancel one another.

Values of F, F_{bond}, and F_{anh} calculated from Eq. (9b) using parameters obtained in several of the fits of Table II are listed in Table IV, along with measured values of F and their separation into F_{bond} and F_{anh} as proposed by the authors.[8] As the separation depends crucially on β, its value as used in each work is also listed. The internal agreement among all measured F's is good. The same holds, to a lesser extent, for the F_{bond} and F_{anh}. Note that all (but one) studies employ a high value of $\beta\approx 3.4$

TABLE IV. Measured and synthesized values of the structure factor, F, and its anharmonic, F_{anh}, and bond-charge, F_{bond}, components for the "forbidden" reflections 442 and 622, in units of millielectrons/atom. Standard deviations are given in the second line of each entry. Values of the anharmonic force constant β employed in separating the components and in the model synthesis are also listed.

		442			622		
	β	F	F_{anh}	F_{bond}	F	F_{anh}	F_{bond}
This work							
b	0	−12.0	0	−12.0	−3.34	0	−3.34
		2.0		2.0	0.62		0.62
c	1.67	−8.10	3.37	−11.5	−0.96	2.22	−3.18
		2.3	0.2	2.3	0.73	0.10	0.72
d	3.38	−4.16	6.84	−11.0	1.47	4.50	−3.03
		2.5	0.22	2.5	0.77	0.14	0.76
p	0	−11.17	0	−11.17	−3.13	0	−3.13
		0.58		0.58	0.18		0.18
q	1.67	−7.61	3.18	−10.79	−0.91	2.09	−3.00
		0.48	0.11	0.47	0.17	0.09	0.15
r	3.38	−3.93	6.46	−10.39	1.35	4.24	−2.89
		0.93	0.12	0.92	0.31	0.10	0.29
Experiment							
Trucano[a]	3.45	−4.38	5.12	−9.50			
		0.25	0.33	0.75			
Mills[b]	3.38	−5.25	4.88	−10.13	±0.63	3.25	−3.88
		0.38	0.50	0.61	0.50	0.38	0.63
Tischler[c]	1.65[d]	−4.63	3.31	−7.91	1.10	1.68	−0.58
	1.41[e]	0.29	0.33	0.44	0.14	0.21	0.25
Tischler[f]	3.38	−4.63	6.95	−11.58	1.10	4.10	−3.00
		0.29	0.33	0.44	0.14	0.21	0.25

[a]Reference 8(c).
[b]Reference 8(d).
[c]Reference 8(b).
[d]For 442.
[e]For 622.
[f]Reference 8(b), as rescaled in Ref. 12.

eV/Å^3, although some neutron and x-ray measurements indicate a lower value of 1.4–1.7 eV/Å^3. The only exception, the work of Tischler and Batterman,[8(b)] was shown by Spackman to yield results strongly conflicting with the refinement analysis. When separated using $\beta=3.38$ eV/Å^3, as given in the last entry of Table IV, F_{bond} and F_{anh} are in excellent agreement with Spackman's analysis as well as with the values derived from other measurements.

A comparison of the measured F values to our synthesized ones shows the best agreement for $\beta=3.38$ eV/Å^3, for which the synthesized F values have the correct sign as well as magnitude. This is in contrast with the strong support provided by the allowed reflection for a lower value of β as discussed above. No explanation can be offered at this time for this dichotomy. Note, however, that the agreement between all the experimental F_{bond}'s and the synthesized ones are good, which lends further credibility to the deformation charge density derived in this study. While no clearcut support for the superiority of the improved model ($p-r$) over the "standard" one ($b-d$) is provided by these results in Table IV, the improved $F_{\text{bond}}(442)$ is somewhat lower than the standard one. Hence, it agrees slightly better with the experimentally derived $F_{\text{bond}}(442)$, which is influenced only a little by the value adopted for β. These results, and the conclusions of Spackman in favor of a high value of β, further indicate the deep need for a better assessment of the relative importance of anharmonic effects.

E. Deformation model dependence

Dawson[9] employed Gaussian, rather than exponential, radial functions to represent the deformation densities:

$$\rho_{3,D}(\mathbf{r})=O_D r^2\exp(-\alpha_D r^2)(xyz/r^3) \tag{10a}$$

and

$$\rho_{4,D}(\mathbf{r})=H_D r^2\exp(-\alpha_D r^2)[(x^4+y^4+z^4)/r^4-\tfrac{3}{5}] . \tag{10b}$$

Fourier transforming, one obtains[9,5]

$$f_3(\mathbf{k})=-O_D A_3 \mathcal{M}_3(k,\alpha_D) \tag{11a}$$

and

$$f_4(\mathbf{k})=H_D A_4 \mathcal{M}_4(k,\alpha_D) , \tag{11b}$$

where

$$\mathcal{M}_n(k,\alpha)=(-k/2)^n\pi^{3/2}\alpha^{-\nu} \times[\Gamma(\nu)/\Gamma(\eta)]M(\nu,\eta,-k^2/4\alpha) . \tag{12}$$

Here $\nu=(5+n)/2$, $\eta=n+\frac{3}{2}$, $\Gamma(x)$ is the usual γ function and $M(a,b,c)$ is the confluent hypergeometric series for which tables[35] and computer routines[36] are available. The model using the same Clementi wave functions employed above for the spherical charge distribution but the Gaussian Eqs. (10)–(12) for the deformation densities is denoted GA in the following.

Although of the wrong asymptotic shape,[37] and leading to divergences in the calculations of higher-order gradients of the microscopic crystal electric field,[38,11(b)] the functions of Eq. (9) were found to represent well the deformation densities of silicon in several studies.[9,14,39] We have, therefore, repeated the full series of fits of Table II for the GA model. The general conclusions derived from the EX model above are fully supported by the GA model fits as well. Again, the best R and GOF parameters are obtained for the fit equivalent to p in Table II. The expansion parameters κ_1 and κ_2 obtained, 0.9955 and 0.9362, are equal within error to those of p in Table III. The same holds for $B_{1,D}=0.4610(17)$ Å^2 and $B_{2,D}=0.00(11)$ Å^2. This indicates that the nonrigid thermal motion, the absence of anharmonic effects, and the expansion of the core L shell, found using the model of Sec. II, are not model-induced artifacts. The best R and GOF values obtained are 0.053 and 1.94, respectively. While this R factor is 40% lower than that of the most recent Gaussian refinement for silicon,[14] it is still almost twice as large as that of the corresponding best refinement using exponentials, p in Table II.

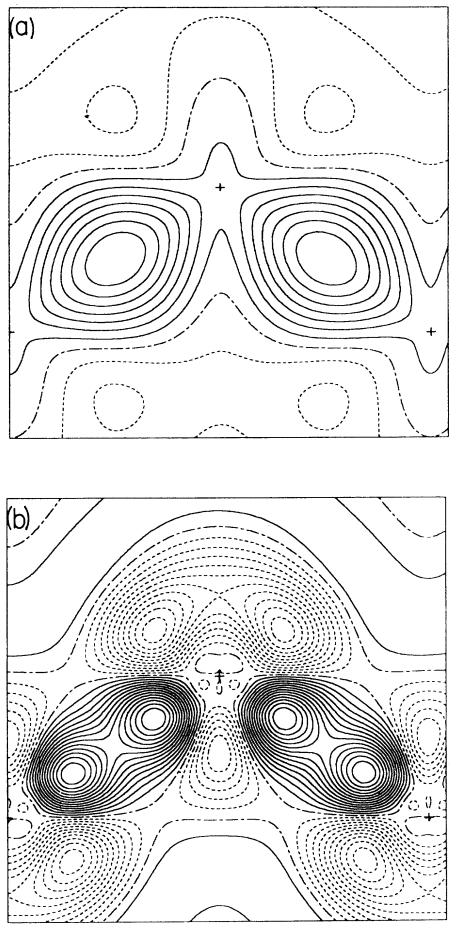

FIG. 3. (a) Same as Fig. 1(a), but using Dawson-type (GA) Gaussian radial functions in the deformation density rather than the Stewart-type (EX) exponentials. (b) Difference between the maps of Figs. 1(a) and 3(a). Contour interval is 0.0015 e/Å^3.

A more detailed assessment of the difference between the two models can be obtained from an examination of the deformation (ρ_{def}) density map in the 110 plane of the GA model, given in Fig. 3(a), and its comparison with that of the EX model, shown in Fig. 1(a). While the general shape is similar, GA yields a less elongated ellipse along the bond direction, and a considerably smaller negative density region behind the atom. The zero-density boundaries are almost identical everywhere except close to the atoms. The map of the difference in ρ_{def} of the two models, given in Fig. 3(b), clearly shows the increased charge concentration in the bond region in EX, at the expense of a larger negative density region mostly, but not only, behind the atoms. The variation of ρ_{def} and its components along the bond, given in Fig. 4, shows, in addition to the different charge concentrations, the narrower maxima and minima of the GA model, which are due to the faster decay of the Gaussian functions as compared to the exponential ones. The peak and dip values are now 0.200 and -0.058 $e/\text{Å}^3$, as compared with 0.221 and -0.068 $e/\text{Å}^3$ for EX. The dip also moved out to $R=1.21$ Å behind the atom as compared to 0.96 Å for EX. These variations result in subtle differences in ρ_{val} as well. The GA ρ_{val} map in Fig. 5 shows the same rectangular bond shape and crescentlike peak above the atom as that of the EX model, Fig. 2(a). The charge distribution along the bond, shown in Fig. 6 reveals, however, that ρ_{val} is practically flat in the midbond region in contrast with the twin-peaked shape of the EX model. The peak height is 26 $me/\text{Å}^3$ lower. Furthermore, both the crescentlike feature above the atom and the saddle behind the atom along the bond direction are higher than in the EX model: 0.354 and 0.298 $e/\text{Å}^3$ as compared to 0.341 and 0.274 $e/\text{Å}^3$, respectively.

Thus, we may summarize that the GA model yields sharper features in the deformation density maps, which is not surprising in view of the sharper Gaussian functions used. It also has a lower density in the bond region, and a higher one almost everywhere else. Finally, the bond has a single flat peak rather than the twin peaks of the EX model. The statistical indices, however, clearly show that the EX model fits the measured data much better, with a 40% smaller R and GOF values.

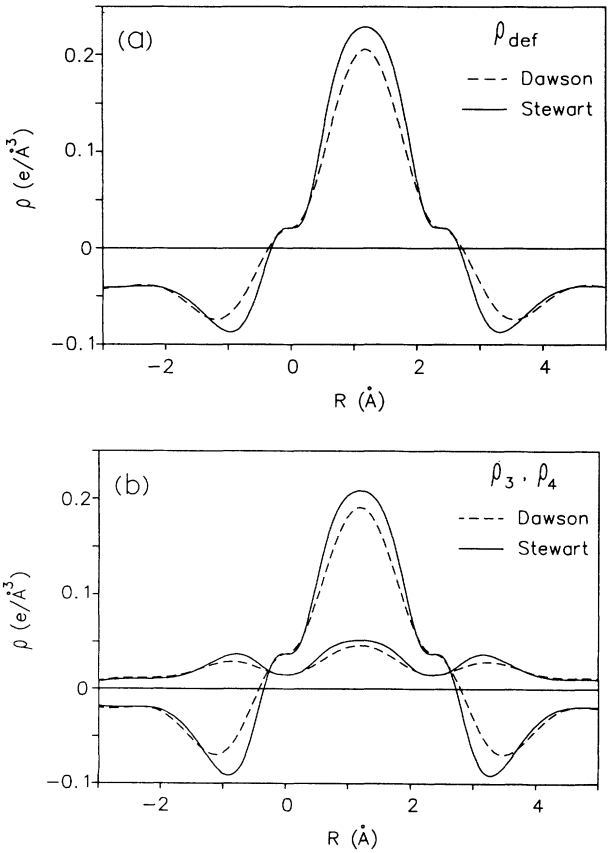

FIG. 4. (a) Deformation charge density and (b) its components along the nearest-neighbor direction, ⟨111⟩, for fit p using the Dawson (GA) and Stewart (EX) models. The silicon atoms are at $R=0$ and 2.3517 Å.

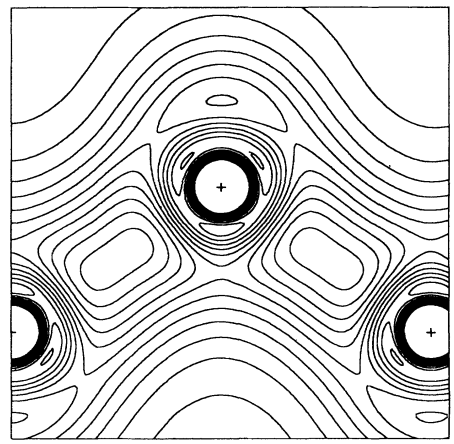

FIG. 5. Valence-charge-density map for the Dawson (GA) model. The units are the same as for Fig. 2(a).

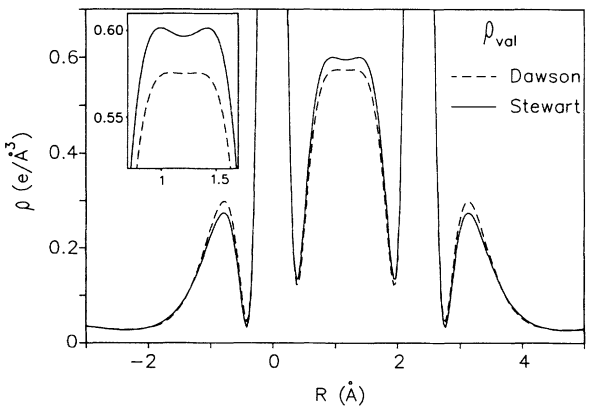

FIG. 6. Valence charge densities along the nearest-neighbor direction, ⟨111⟩, for fits p for Dawson (GA) and Stewart (EX) models. A magnified view of the midbond region is shown in the inset.

F. Wave function dependence

As mentioned above, the free-atom form factors used in the present study were those obtained from the Hartree-Fock (HF) wave functions of Clementi,[31] which are generally considered to be among the best for silicon. This choice has several advantages. First, it puts our results on equal footing with previous refinements, almost all of which use the same wave functions.[1,9,10,12,26,39] Moreover, Clementi's tables allow for the calculation of shell-by-shell form factors which are essential for this study. Other calculations, like those of Ref. 40 and the bound-atom *ab initio* calculations, provide only neutral-atom form factors or Si^{4+} "core" ones at most. To test the sensitivity of our results to the wave functions employed, we repeated the sequence of fits of Table II using the improved set of wave functions of Clementi and Roetti[41] instead of the Clementi[31] ones. In all cases, identical R and GOF values were obtained and the redefined parameter values deviated from the previous ones by less than $\pm 0.3\sigma$. As no relativistic shell-by-shell structure factors of silicon are available in the literature, the influence of relativistic effects could not be checked. However, Cromer[42] has shown in a detailed comparative study that the differences between f values obtained from nonrelativistic HF wave functions and those obtained from relativistic Dirac-Slater ones are negligibly small for atomic numbers below 25. Furthermore, "standard" model fits, similar to those of $b-d$ in Table II were carried out by PMM and Fehlmann,[14] using relativistic HF wave functions.[40,43] The close agreement of their results with those obtained from nonrelativistic HF wave functions in R, GOF, and the final values of the parameters refined, strongly supports the conclusion that relativistic effects are negligible for silicon even for high-accuracy studies like the present one.

We conclude, then, that the effects discovered in this study are most probably real and not artifacts due to insufficiently refined wave functions. A direct test of relativistic effects on our conclusions, though most desirable, will have to await the availability of high-quality relativistic wave functions and corresponding shell-by-shell atomic form factors f_{nl}. Similarly, an understanding of the role played by, and the importance of the exchange potential and correlation effects also awaits theoretical progress.

V. CONCLUSIONS

A detailed analysis of the charge distribution in crystalline silicon is presented. It is based on the best available set of low-order structure factors recently published by Cummings and Hart,[2] and one datum by Alkire *et al.*[6] The multipole expansion formalism is employed to account for crystal bonding deformations. Allowance is made for expansion of shells other than the valence shell and for different thermal motion of the valence and core shells. The best model is found to describe the data to its limit of accuracy, with an R factor two- to threefold smaller than previous studies. The main features discovered are the following.

(i) $A \sim 0.5\%$ spherical expansion of the L shell. This is in addition to the $\sim 6\%$ expansion of the M shell, also found in earlier studies. This strongly supports an unproved suggestion by Spackman.[12]

(ii) A much reduced thermal vibrational amplitude for the valence shell, indicated by a Debye parameter $B_2 \leq 0.11$ Å^2. While the value derived for B_2 is smaller than some of the predictions, the effect itself is supported by high-order-reflection x-ray, electron channeling, and some of the "forbidden" reflection measurements.

(iii) An anharmonic force constant $\beta \leq 0.7$ eV/Å^3 at a 1σ confidence level. On this level, it is smaller by a factor of 2 than the smallest neutron result, but is strongly supported by high-order reflection x-ray measurements. On a more conservative 2σ level, our results agree marginally with the lowest neutron result but still disagree with the higher "forbidden" reflection derived values.

The last conclusion, though strongly supported by the fit results, leads to calculated "forbidden" $F(442)$ and $F(622)$ structure factors which disagree with the measured ones. These, in turn, rather support a $\beta = 3.38$ eV/Å^3. While this dichotomy requires future study and clarification, it has no bearing on the other conclusions, which remain unchanged regardless of the value adopted for β, as discussed in Sec. IV A.

The at-rest deformation and valence charge densities derived from the model are found to be in good agreement with recent experimentally derived results. The agreement with *ab initio* calculations is improved particularly in the midbond region. The Stewart-type exponential radial functions are shown to be superior to the Gaussian Dawson-type ones for faithfully reproducing the deformation density.

This study indicates that more work is required, in particular, in ascertaining the role played by, and importance of relativistic, exchange, and correlation effects in the wave functions. Theoretical prerequisites for further progress are the availability of highly accurate shell-by-shell f_{nl} values obtained from wave functions including the effects mentioned above. On the experimental side, the resolution of the discrepancies among presently available values of β is essential. Perhaps an independent, unambiguous experimental determination is called for.

ACKNOWLEDGMENTS

My sincerest thanks to Michael Hart for his invariably helpful advice, numerous stimulating discussions, and for critical reading of the manuscript. The generous assistance of P. Sommer-Larsen in supplying copies of his free-atom structure programs is gratefully acknowledged, as is G. Zipori's expert computer programming. This work was supported by SERC, U.K.

[1]P. J. E. Aldred and M. Hart, Proc. R. Soc. London, Ser. A **332**, 223 (1973); **332**, 239 (1973).
[2]S. Cummings and M. Hart, Aust. J. Phys. **41**, 423 (1988).
[3]R. Teworte and U. Bonse, Phys. Rev. B **29**, 2102 (1984).
[4]T. Saka and N. Kato, Acta Crystallogr. A **42**, 469 (1986).
[5]M. Deutsch and M. Hart, Phys. Rev. B **31**, 3846 (1985).
[6]R. W. Alkire, W. B. Yelon, and J. R. Schneider, Phys. Rev. B **26**, 3097 (1982).
[7]J. B. Roberto, B. W. Batterman, and D. T. Keating, Phys. Rev. B **9**, 2590 (1974).
[8](a) J. B. Hastings and B. W. Batterman, Phys. Rev. B **12**, 5580 (1975); (b) J. Z. Tischler and B. W. Batterman, *ibid.* **30**, 7060 (1984); (c) P. Trucano and B. W. Batterman, *ibid.* **6**, 3659 (1972); (d) D. Mills and B. W. Batterman, *ibid.* **22**, 2887 (1980).
[9]B. Dawson, Proc. R. Soc. London, Ser. A **298**, 255 (1967); **298**, 379 (1967).
[10]Y. W. Yang and P. Coppens, Solid State Commun. **15**, 1555 (1974).
[11](a) P. F. Price, E. N. Maslen, and S. L. Mair, Acta Crystallogr. A **34**, 183 (1978); (b) P. F. Price and E. N. Maslen, *ibid.* **34**, 173 (1978).
[12]M. A. Spackman, Acta Crystallogr. A **42**, 271 (1986).
[13]C. Scheringer, Acta Crystallogr. A **36**, 205 (1980).
[14]M. Fehlmann, J. Phys. Soc. Jpn. **47**, 225 (1979).
[15]D. R. Hamann, Phys. Rev. Lett. **42**, 662 (1979).
[16](a) M. T. Yin and M. L. Cohen, Phys. Rev. Lett. **45**, 1004 (1980); (b) Phys. Rev. B **26**, 5668 (1982); (c) Phys. Rev. Lett. **50**, 1172 (1983); (d) A. Zunger and M. L. Cohen, Phys. Rev. B **20**, 4082 (1979).
[17](a) J. Chelikowsky and M. L. Cohen, Phys. Rev. Lett. **33**, 1339 (1974); Phys. Rev. B **10**, 5095 (1974); (b) J. R. Chelikowsky and S. G. Louie, *ibid.* **29**, 3470 (1983); W. Y. Ching and B. N. Harmon, *ibid.* **34**, 5305 (1986); F. Zandiehnadem and W. Y. Ching, *ibid.* **41**, 12 162 (1990).
[18]H. Aourag *et al.*, Phys. Status Solidi B **156**, 497 (1990).
[19]C. S. Wang and B. M. Klein, Phys. Rev. B **24**, 3393 (1981); in *Electron Distributions and the Chemical Bond,* edited by P. Coppens and M. B. Hall (Plenum, New York, 1982).
[20](a) H. M. Polatoglou and M. Methfessel, Phys. Rev. B **41**, 5898 (1990); (b) M. Methfessel, C. O. Rogriguez and O. K. Andersen, *ibid.* **40**, 2009 (1989); (c) K. H. Weyrich, *ibid.* **37**, 10 269 (1988); (d) O. K. Andersen, Z. Pawlowska, and O. Jepsen, *ibid.* **34**, 5253 (1986), and references therein.
[21]P. Hohenberg and W. Kohn, Phys. Rev. **136**, B864 (1964); W. Kohn and L. J. Sham, *ibid.* **140**, A1133 (1965).
[22]M. Deutsch, M. Hart, and P. Sommer-Larsen, Phys. Rev. B **40**, 11 666 (1989).
[23]L. V. Hau, E. Laegsgaard, and J. U. Andersen, Nucl. Instrum. Methods Phys. Res. B **48**, 244 (1990); J. U. Andersen, E. Laegsgaard, and A. H. Sørensen, Nucl. Instrum. Methods B **2**, 63 (1984); H. Park *et al.*, Phys. Rev. B **35**, 13 (1987).
[24]R. F. Stewart, J. Chem. Phys. **58**, 1668 (1973); Acta Crystallogr. A **32**, 565 (1976).
[25]R. F. Stewart, in *Electron and Magnetization Densities in Molecules and Crystals,* edited by P. Becker (Plenum, New York, 1980), pp. 405, 427, 439.
[26]N. K. Hansen and P. Coppens, Acta Crystallogr. A **34**, 909 (1978), and references therein.
[27]P. Coppens *et al.*, Acta Crystallogr. A **35**, 63 (1979).
[28]M. Deutsch and M. Hart, Phys. Rev. B **30**, 640 (1984); **37**, 2701 (1988).
[29]P. R. Bevington, *Data Reduction and Error Analysis for the Physical Sciences* (McGraw-Hill, New York, 1969), Chap. 5.
[30]H. Hattori, H. Kuriyama, T. Kategawa, and N. Kato, J. Phys. Soc. Jpn. **20**, 988 (1965).
[31]E. Clementi, IBM J. Res. Dev. **9**, Suppl. 2 (1965).
[32]Z. Su and P. Coppens, J. Appl. Cryst. **23**, 71 (1990).
[33]I. Fujimoto, Phys. Rev. B **9**, 591 (1974).
[34]D. Keating, A. Nunes, B. Batterman, and J. Hastings, Phys. Rev. B **4**, 2472 (1971); J. B. Roberto and B. W. Batterman, *ibid.* **2**, 3220 (1970).
[35]M. Abramowitz and I. A. Stegun, *Handbook of Mathematical Functions* (Dover, New York, 1972), Chap. 13.
[36]For example, Routine C235, Centre d'Etudes Recherche Nucleaires Subroutine Library (Geneva, Switzerland).
[37]V. H. Smith, Jr., in *Electron Distributions and the Chemical Bond,* edited by P. Coppens and M. B. Hall (Plenum, New York, 1982), p. 3.
[38]R. F. Stewart, J. Chem. Phys. **58**, 4430 (1973).
[39]J. F. McConnell and P. L. Sanger, Acta Crystallogr. A **26**, 83 (1970).
[40]D. T. Cromer and J. T. Waber, in *International Tables for X-Ray Crystallography,* edited by J. A. Ibers and W. C. Hamilton (Kynoch, Birmingham, 1974), Vol. IV, Chap. 2.2.
[41]E. Clementi and C. Roetti, At. Data Nucl. Data Tables **14**, 177 (1974).
[42]D. T. Cromer, Acta Crystallogr. **19**, 224 (1965).
[43]M. A. Coulthard, Proc. Phys. Soc. **91**, 44 (1967); P. A. Doyle and P. S. Turner, Acta Crystallogr. A **24**, 390 (1968).